Progress In Electromagnetics Research M, Vol. 72, 125–133, 2018

A Rotating-magnet Based Mechanical Antenna (RMBMA) for ELF-ULF Wireless Communication

Shuhong Gong[1, *], Yu Liu[1], and Yi Liu[2]

Abstract—This paper presents some theoretical and experimental analyses of the rotating-magnet based mechanical antenna (RMBMA), a promising portable transmitting antenna for ELF-ULF (3–3000 Hz) wireless communication. Based on the Amperian current model, a theoretical model is developed to analyze the electromagnetic fields generated by RMBMA. A prototype is manufactured and measured, and the measurements coincide well with the calculations based on the established theoretical model. The results reveal that this new technique can create a constant channel condition in complex propagation environment, and an RMBMA with a small size can produce an AC magnetic field of 1 pT at hundreds of meters across lossy media, such as soil and sea water.

1. INTRODUCTION

Radio waves with frequencies from extremely low frequency (ELF, 3 Hz–30 Hz) to ultra-low frequency (ULF, 300 Hz–3 KHz) band have small path losses in water and soil; therefore, they play irreplaceable roles in the fields of underwater and underground communication, such as submarine communication, mine emergency communication, and earthquake prediction. However, a traditional ELF-ULF antenna has a very large size due to the very long operating wavelength (10^2 km–10^5 km), which has hindered its wide application [1, 2]. Recently, the Defense Advanced Research Projects Agency (DARPA) has proposed A Mechanically Based Antenna (AMEBA), which generates low frequency electromagnetic waves by mechanically moving charge carriers or magnetic materials [3–5]. Mechanical antenna is a promising miniaturized antenna for low frequency (such as ELF-ULF) communication, since its size does not need to be in the same order of magnitude as the operating wavelength to effectively carry the standing current wave.

Rotating-magnet is a feasible structure for a mechanical antenna. In 2009, Liu was granted a patent on a new antenna that uses rotating permanent magnets to generate low-frequency electromagnetic waves [6]. Then in 2017, Majid proposed an underwater positioning system composed of at least three mechanical antennas as reference points and a multi-dimensional vector magnetometer on the UUV as the receiver [4]. Under the assumption that the magnetic field generated by a time-varying dipole has the same spatial distribution as that of a static dipole, Madanayake et al. derived the magnetic field expression of mechanically rotating dipoles, but their theoretical analyses ignore the conversion between magnetic field and electric field [7]. In [8, 9], it is concluded that a spinning magnet system is not subject to Chu Harrington limit in ULF communications, and the electromagnetic fields expression in the far field is obtained, but there is no study of that in the near field.

Currently, researches on rotating-magnet based mechanical antennas are still in an exploratory stage. No mature theoretical model has been formed yet, and there is no experimental measurement. In this paper, a permanent magnet is equivalent to the Amperian current on its surface, and the direction

Received 2 July 2018, Accepted 13 August 2018, Scheduled 22 August 2018

* Corresponding author: Shuhong Gong (shgong@xidian.edu.cn).

[1] School of Physics and Optoelectronic Engineering, Xidian University, Xi'an, China. [2] School of Telecommunications Engineering, Xidian University, Xi'an, China.

and location of the current change along with the mechanical motion of the magnet. We first solve the retarded potential generated by the time-varying electric current and then calculate the electrical field and magnetic field using the retarded potential. According to the numerical analysis, we find that most of the electromagnetic energy of the RMBMA is not really radiated, but it is statically stored in the field surrounding the antenna, as a static field of a permanent magnet, it will not be reflected on the interface between the two different media. An RMBMA can be used to communicate with a receiving loop antenna by magnetic induction, which can create constant channel conditions when the propagation media are air, water and most kinds of soil, since the magnetic permeabilities of these media are similar [10, 11]. So the ELF-ULF band RMBMA is applicable to underwater communication, underground communication and communication in mixed media of air, soil and water in the near field.

A prototype was manufactured using a permanent magnet with a size of 10 cm × 5 cm × 2 cm. Its near-field pattern is measured by a ferrite-loaded loop in the plane through the shaft, and it coincides well with the simulation results. The measurement in the propagation media of air and salt water shows that the interface reflection is negligible.

The remainder of this paper is organized as follows. In Section 2, the mathematical expressions of the electromagnetic fields generated by the RMBMA are derived. In Section 3, the range dependence and directional dependence of the field generated by RMBMA are simulated and analyzed. In Section 4, a prototype is manufactured and measured in the near field. Finally, the paper is concluded in Section 5.

2. THEORETICAL MODEL OF RMBMA

If a permanent magnet is mechanically moving, the magnetic field will change over time. According to Maxwell's equations, there will be a mutual conversion between magnetic field and electric field, and then the electromagnetic wave is produced, which is how an RMBMA works. The Cartesian coordinate system is established with the center of the magnet as the origin for convenience. The z-axis coincides with the shaft, and the angle between the magnetization direction and z-axis at the beginning of rotation is denoted by Φ_0, as shown in Figure 1.

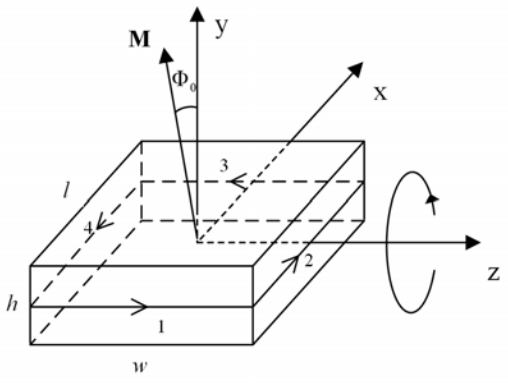

Figure 1. The sketch of the rotating magnet of the RMBMA.

According to the Amperian current model, from a macro perspective, a uniformly magnetized permanent magnet is equivalent to the Amperian current on its surface [12–14], and the equivalent surface current density $\boldsymbol{\alpha}$ is given as

$$\boldsymbol{\alpha} = \mathbf{M} \times \hat{n} \tag{1}$$

where $\mathbf{M}$ is the magnetization vector of magnetic body, and $\hat{n}$ is the normal unit vector oriented from magnetic body to transmission medium. (In this paper, the vector is represented by a boldfaced letter, and the same letter in non bold format represents the magnitude of the vector.) Generally, the surface current is quite high, but we need not worry that it will produce Joule heat, because it is not a real current but a macroscopic performance of magnetic moments of the molecular or atomic particles in permanent magnet material. In Figure 1, the surface current is distributed on the four square sides of

the cuboid magnet (labeled as 1, 2, 3, 4 in the Figure 1) parallel to the magnetization direction, and there is no surface current on the other two sides.

To compute the radiation field generated by time-varying current, we can first calculate the magnetic potential $\mathbf{A}$ of field point $\mathbf{r}$ at time t,

$$\mathbf{A}(\mathbf{r},t) = \frac{\mu}{4\pi}\iiint_V \frac{\mathbf{J}(\mathbf{r}',t-R/c)}{R}dv' \tag{2}$$

where μ is the permeability of the transmission medium, R the distance between field point $\mathbf{r}$ and source point $\mathbf{r}'$, which is given by $R=|\mathbf{r}-\mathbf{r}'|$, c the speed of light, and $\mathbf{J}(\mathbf{r}',t-R/c)$ the volume current density of source point $\mathbf{r}'$ at time $t'=t-R/c$. For a rotating permanent magnet as a source of radiation, the equivalent current is only distributed on its surface, and the retarded potential $\mathbf{A}$ is given as [15]

$$\mathbf{A}(\mathbf{r},t) = \frac{\mu}{4\pi}\iint_{\Omega(t)} \frac{\boldsymbol{\alpha}(\mathbf{r}',t-R/c)}{R}ds \tag{3}$$

The integral domain $\Omega(t)$ is the surface of the permanent magnet with equivalent current, i.e., the four sides marked 1, 2, 3, 4 in Figure 1. The equivalent surface current density is a constant equal to M, but the direction of current flow is time-varying. Assume that the cuboid permanent magnet has a length of l, width of w, height of h, and it rotates at an angular velocity ω, as shown in Figure 1, then

$$\begin{aligned}\mathbf{A}(\mathbf{r},t) \;=\; & \mu\alpha/(4\pi)\int_{-w/2}^{w/2}\int_{-h/2}^{h/2}\hat{z}/|\mathbf{r}-(-l\hat{l}/2+\xi\hat{z}+\zeta\hat{h})|d\xi d\zeta + \\ & \mu\alpha/(4\pi)\int_{-l/2}^{l/2}\int_{-h/2}^{h/2}\hat{l}/|\mathbf{r}-(w\hat{z}/2+\xi\hat{l}+\zeta\hat{h})|d\xi d\zeta - \\ & \mu\alpha/(4\pi)\int_{-w/2}^{w/2}\int_{-h/2}^{h/2}\hat{z}/|\mathbf{r}-(l\hat{l}/2+\xi\hat{z}+\zeta\hat{h})|d\xi d\zeta - \\ & \mu\alpha/(4\pi)\int_{-l/2}^{l/2}\int_{-h/2}^{h/2}\hat{l}/|\mathbf{r}-(-w\hat{z}/2+\xi\hat{l}+\zeta\hat{h})|d\xi d\zeta\end{aligned} \tag{4}$$

The four terms in Equation (4) correspond to the integrals in the four sides 1, 2, 3, and 4 of the permanent magnet in Figure 1, respectively. $\hat{z}$, $\hat{l}$ and $\hat{h}$ are unit vectors along the z-axis, edge l and edge h of the cuboid permanent magnet at time $t'=t-R/c$, respectively, and $\hat{l}$ and $\hat{h}$ are functions of time t

$$\hat{l} \;=\; (1,j,0)e^{-j\omega t'-j\Phi_0} = (1,j,0)e^{j(kR-\omega t)-j\Phi_0} \tag{5}$$

$$\hat{h} \;=\; (-j,1,0)e^{-j\omega t'-j\Phi_0} = (-j,1,0)e^{j(kR-\omega t)-j\Phi_0} \tag{6}$$

where k is the wave number, given by $k=\omega/c$. Generally, the communication distance is much larger than the size of the permanent magnet, i.e., $r \gg r'$, under this condition,

$$\frac{1}{R} \;\approx\; \left[1+\frac{\mathbf{r}'\cdot\hat{r}}{r}\right] \tag{7}$$

$$e^{jkR} \;\approx\; e^{jkr}(1-jk\mathbf{r}'\cdot\hat{r}) \tag{8}$$

The retarded potential $\mathbf{A}$ can be deduced by solving Equations (3)–(8):

$$\mathbf{A}(\mathbf{r},t) = B_0Ve^{-j\Phi_0}\frac{e^{j(kr-\omega t)}}{4\pi r^3}\left[-\hat{z}(x+jy)+\;(\hat{x}+j\hat{y})z(1-jkr)\right] \tag{9}$$

where B_0 and V are respectively remanence and volume of the permanent magnet, and $B_0=\mu M$.

The magnetic field $\mathbf{B}(\mathbf{r},t)$ generated by RMBMA can be calculated using the definition of the retarded potential $\mathbf{A}$, and then the electric field $\mathbf{E}(\mathbf{r},t)$ can be derived by $\mathbf{B}(\mathbf{r},t)$

$$\begin{aligned}\mathbf{B}(\mathbf{r},t) =& \nabla\times\mathbf{A}(\mathbf{r},t) \\ =& \frac{B_0Ve^{j(kr-\omega t)}}{4\pi r^3}\Big\{-\hat{r}(2j+kr)\sin\theta+\hat{\theta}(j+2kr-jk^2r^2)\cos\theta+ \\ & \hat{\phi}\;[-1+(2jkr+k^2r^2)\cos^2\theta]\Big\}e^{j(\phi-\Phi_0)}\end{aligned} \tag{10}$$

$$\begin{aligned}\mathbf{E}(\mathbf{r},t) =& \frac{j}{\omega\epsilon\mu}\nabla\times\mathbf{B}(\mathbf{r},t)\\ =& \frac{\eta MVe^{j(kr-\omega t)}}{4\pi r^3}\left\{\hat{r}\frac{3}{2}(2-jkr)\sin 2\theta+\hat{\theta}(-2+2jkr+k^2r^2)\cos^2\theta+\right.\\ & \left.\hat{\phi}(-2j-2kr+jk^2r^2)\cos\theta\right\}e^{j(\phi-\Phi_0)}\end{aligned} \tag{11}$$

where $\eta=\sqrt{\mu/\epsilon}$ is the wave impedance of transmission medium. For the convenience to analyze the characteristics of fields, they are calculated in a spherical coordinate system, where θ is the polar angle measured from the positive direction of z-axis, and ϕ is the azimuth angle of orthogonal projection of radius vector $\mathbf{r}$ on x-y plane.

3. SIMULATION AND ANALYSES

The ELF-ULF band electromagnetic waves are more suitable than RF waves for lossy media, such as soil and water, because of less skin effects due to the lower frequency. The complex dielectric permittivity of conductive medium in ELF-ULF band is $\epsilon=\epsilon'+j\sigma/\omega$, where σ is the electrical conductivity of medium. Accordingly, the wave number is also a complex number $k=k_R+jk_I$. k_R and k_I are given by

$$k_R=\omega\sqrt{\frac{\mu\epsilon'}{2}}\sqrt{\sqrt{1+\left(\frac{\sigma}{\omega\epsilon'}\right)^2}+1} \tag{12}$$

$$k_I=\omega\sqrt{\frac{\mu\epsilon'}{2}}\sqrt{\sqrt{1+\left(\frac{\sigma}{\omega\epsilon'}\right)^2}-1} \tag{13}$$

The B-fields in air, soil and sea water are evaluated using MATLAB according to Eqs. (10), (12) and (13). The results are shown in Figure 2. In our simulation, the volume of permanent magnet is $0.0001\,m^3$, and its remanence is 1.2 T (tesla). The soil composition is set as follows. The proportion of clay, silt, and sand is 13 : 29 : 58, and the volumetric water content is 15%, which are typical values in nature, and its conductivity and real part of relative permittivity are about 0.015 S/m and 10, respectively [16, 17]. The parameters of sea water are set as follows. The salinity is 3.5%; the temperature is 10 degrees Celsius; its conductivity and real part of relative permittivity are about 3.8 S/m and 81, respectively [18]. The magnetic permeabilities of air, soil and sea water are almost the same as that of vacuum, which is $4\pi\times10^{-7}$ H/m. The ELF-ULF waves are usually received by small receiving loops through magnetic induction, so the intensity of the magnetic field is used to evaluate the electromagnetic wave generated by RMBMA.

In Figure 2, the magnetic fields generated by RMBMA are shown in pT (picotesla) versus the transmission distance r with different media of air, soil and sea water. As expected, the path losses caused by conduction currents are affected by media conductivity and operating frequency, the higher the conductivity of the medium or the higher the operating frequency, the greater the path losses. On the other hand, there is an anomaly that the B-field in the conductive medium is greater than that in the air within a certain distance, because the module value of wave number k will be larger due to the conductivity, then the path losses will be reduced according to Eqs. (10) and (11). However, as the distance r is further increased, the losses due to the conduction currents will play major roles, and the electromagnetic fields in the conductive medium will be rapidly attenuated.

Assume that the minimum signal intensity that the receiver can detect is 1 pT, when the operating frequency is 30 Hz, the maximum communication distances are 238.2 m in air, 264.8 m in soil and 203.5 m in sea water, respectively. When the operating frequency is 300 Hz, the maximum communication distances are 238.2 m in air, 294.9 m in soil and 106.9 m in sea water, respectively. Some ELF-ULF receivers reported can detect magnetic signal lower than 1 fT (femtotesla) [19, 20]. The maximum communication distance will be up to 481.9 m in sea water at 30 Hz if the receiver sensitivity is 1 fT. In a word, the simulation results show that the rotating-magnet based mechanical antenna with a permanent magnet with the volume of $0.0001\,\mathrm{m}^3$ can achieve communication within hundreds of meters in soil or sea water.

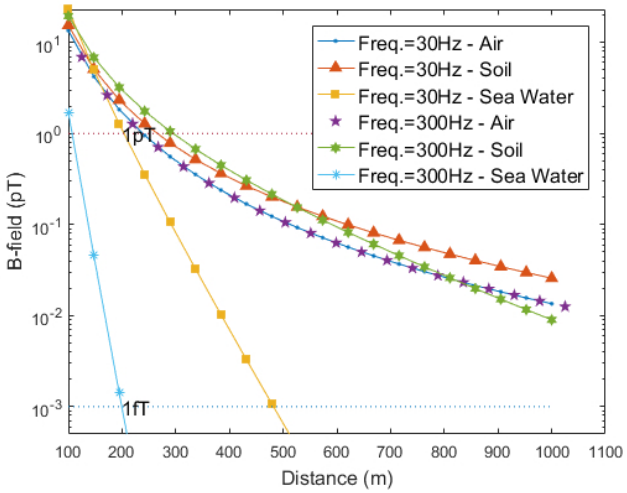

Figure 2. AC magnetic fields of RMBMA with different operating frequency and propagation media.

From the above simulation results, it is known that the communication distances using an RMBMA are much smaller than its operating wavelengths. Therefore, it is more valuable to study the near-field characteristics of the antenna. According to Eqs. (10) and (11), in the near field ($kr \ll 1$), the Poynting vector is almost perpendicular to the radial vector $\hat{r}$, so most of the electromagnetic energy produced by the antenna is not radiated far away, but it is statically stored in the field surrounding the antenna. Therefore, the normalized near-field pattern of magnetic field rather than the radiation pattern is simulated, and it is defined as the field strength at a constant radius divided by the maximum value.

$$B(\theta,\phi) = \frac{B(\theta,\phi)}{B(\theta,\phi)_{\max}}, \quad \text{when } r = r_0 \ll \lambda \tag{14}$$

According to Eqs. (10) and (14), the near-field B pattern is drawn using MATLAB as shown in Figure 3. As we can see from Figure 3, the B-field strength in the direction along the rotation shaft ($\theta = 0°$) is minimum. As θ increases, the B-field gradually increases and reaches a maximum when the $\theta = 90°$, and the ratio of the minimum and maximum magnetic field is $\sqrt{2/5}$. According to Eq. (8), the angle ϕ does not affect the B-field intensity but its phase, which is caused by the symmetry of the rotating-magnet body. Therefore, RMBMA is an omnidirectional antenna.

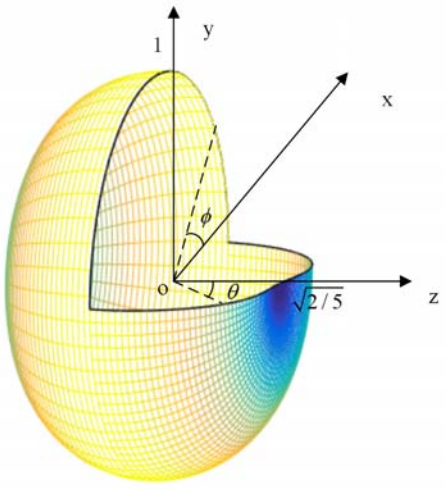

Figure 3. Simulated near-field B diagram of the RMBMA.

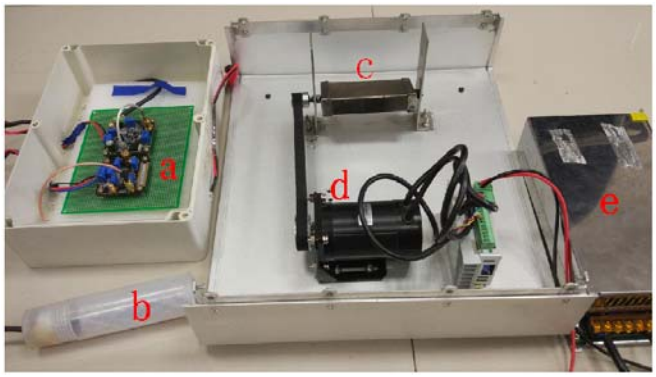

Figure 4. Photograph of prototype and magnetic field receiver, including: (a) circuits of amplifier and low pass filter, (b) a ferrite-loaded receiving loop with waterproof materials, (c) magnetic body, (d) DC motor, (e) DC power supply.

4. EXPERIMENTAL VERIFICATION

A prototype of RMBMA is designed and manufactured, using a neodymium magnet with a remanence of 1.2 T, with a size of 10 cm × 5 cm × 2 cm (volume: 0.0001 m^3). A ferrite-loaded loop is adopted as receiving antenna. The receiving signal is amplified 500 times and filtered by a four order Chebyshev low-pass filter with a cutoff frequency of 100 Hz before being displayed on the oscilloscope. Figure 4 shows a photograph of prototype and magnetic field receiver. Figure 5 shows the waveform of receiving voltage (with noise) in time domain.

The amplitudes of $\mathbf{B}_r$ and $\mathbf{B}_\phi$ are measured versus transmission distance r in a certain angle of $\theta = 90°$ as shown in Figure 6. In the test, the salinity of salt water is 3.5%; the rotating-magnet based mechanical antenna is located at 0.6 m above the water surface; the amplitudes of $\mathbf{B}_r$ and $\mathbf{B}_\phi$ are measured from air to water by the ferrite-loaded loop. It can be observed from Figure 5 that the measurements are well consistent with the calculations in both air and salt water, which validates the theoretical model established in Section 2 to some extent.

It is noteworthy that there is no observable reflection of the magnetic field at the surface of the water.

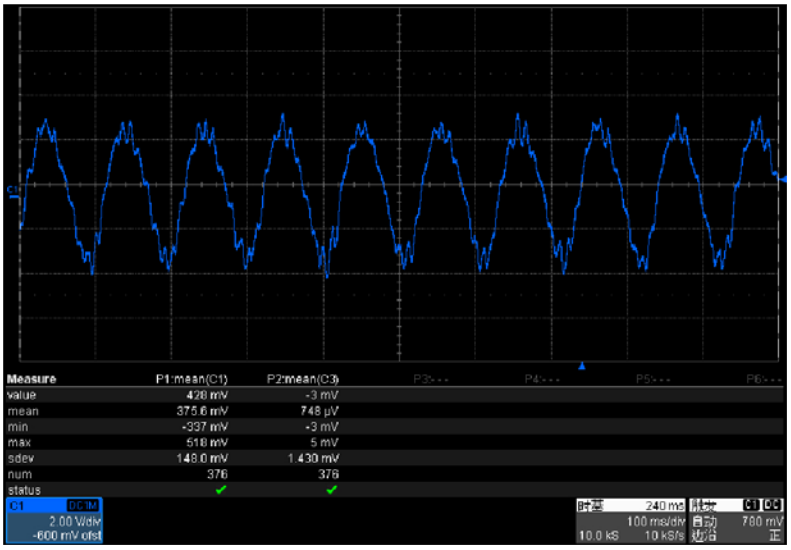

Figure 5. Time domain waveform of receiving voltage generated by AC magnetic signal (with noise).

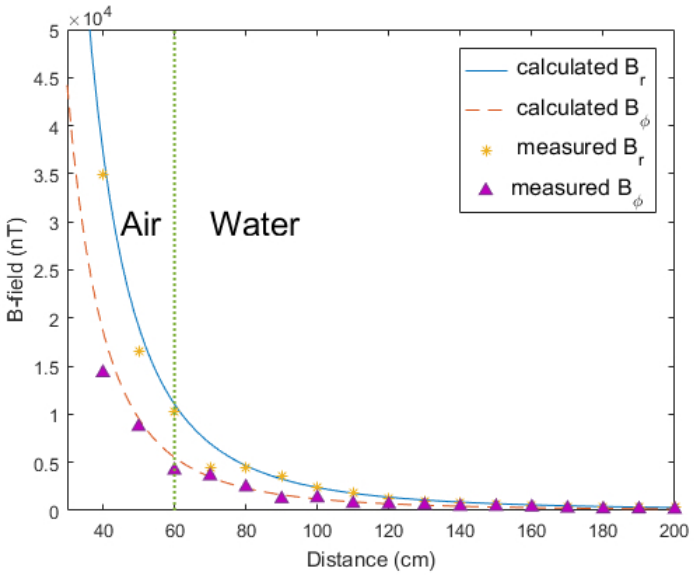

Figure 6. The measured and calculated B-field in air-water mixed media.

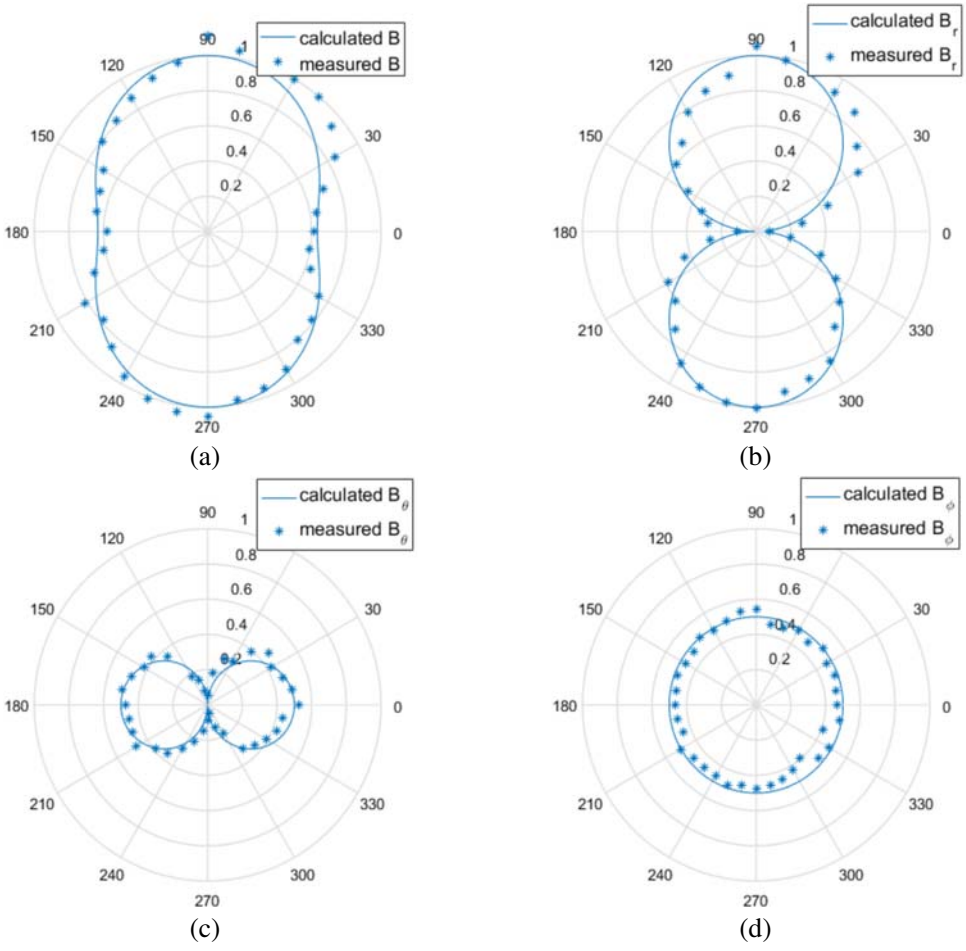

Figure 7. The measured and simulated near-field pattern of field B and its three orthogonal components: B_r, B_θ and B_ϕ.

This is because the transmitting antenna communicates with the receiving loop by magnetic induction, which is mainly carried by the non-radiative magnetic field in the near-field. It exists as an energy statically stored close to the transmitting antenna, such as the static magnetic field of a permanent magnet, so it will not be reflected on the interface between two different media. On the other hand, because the magnetic permeabilities of soil and water are similar to that of air, the magnetic field does not refract when passing through the interfaces of theses media, and the channel conditions of these media for magnetic induction communication are almost the same. These are the advantages of the RMBMA in communication across different media.

The measured near-field B pattern is drawn, which refers to the normalized measured B-field at the radius of 2 m versus θ, and the simulated pattern is plotted in the same figure for comparison, as shown in Figure 7. In Figure 7(a), the measured amplitudes of B-field are drawn by asterisks and simulated amplitudes of B-field drawn by a solid line (it has the same shape as the profile of Figure 3). All the B-fields are normalized by being divided by the maximum simulated value. Figure 7(b), Figure 7(c) and Figure 7(d) show the near-field patterns of B_r, B_θ and B_ϕ, respectively, and all of them are normalized by being divided by simulated value of B_r in the direction of $\theta = 0°$, in order to compare the amplitudes of the three components more intuitively. The measurements coincide well with the calculations, which further validates the theoretical model established in Section 2.

5. CONCLUSION

The electromagnetic field expressions of rotating-magnet based mechanical antenna are derived based on the Amperian current model. A prototype was manufactured using the magnet with the size of 10 cm × 5 cm × 2 cm, and the AC magnetic fields within 2 meters were measured, which coincide well with calculations. According to the theoretical and experimental results of this paper, some characteristics of the RMBMA are shown as follows.

- RMBMA is an omnidirectional antenna. A small size RMBMA can realize communication within hundreds of meters in soil or sea water. For example, the RMBMA with a permanent magnet with the volume of 0.0001 m^3 and the remanence of 1.2 T can produce magnetic field signal of 1 pT at 264.8 m across soil ($\epsilon' = 10\epsilon_0, \sigma = 0.015$ S/m) and 203.5 m across sea water ($\epsilon' = 81\epsilon_0, \sigma = 3.8$ S/m), when the operating frequency is 30 Hz.
- The channel condition is almost constant when RMBMA communicates with receiving loop by magnetic induction in air, water and most kinds of soil, because the permeabilities of these media are similar.

Currently, the study on RMBMA is still in an infant stage. There are still many problems to be solved, such as the practical structure of the motion control system, signal loading technology, and compatibility between RMBMA and traditional antenna in one wireless system.

ACKNOWLEDGMENT

The authors would like to thank the support of the National Natural Science Foundation of China (Grant No. 61771375). They would also like to thank Hu Zhao, Xintong Zhang, Hao Yang and Wenhao Hao for their help during the experiment.

REFERENCES

1. Liu, C., L. G. Zheng, and Y. P. Li, "Study of elf electromagnetic fields from a submerged horizontal electric dipole positioned in a sea of finite depth," *2009 3rd IEEE International Symposium on Microwave, Antenna, Propagation and EMC Technologies for Wireless Communications*, 152–157, Beijing, China, Oct. 2009.
2. Barr, R., W. Ireland, and M. J. Smith, "Elf, Vlf and Lf radiation from a very large loop antenna with a mountain core," *Microwaves Antennas & Propagation IEE Proceedings H*, Vol. 140, No. 2, 129–134, 1993.

3. Bickford, J. A., R. S. McNabb, P. A. Ward, et al., "Low frequency mechanical antennas: Electrically short transmitters from mechanically-actuated dielectrics," *Antennas and Propagation & USNC/URSI National Radio Science Meeting*, 1475–1476, San Diego, USA, Jul. 2017.
4. Manteghi, M., "A navigation and positioning system for unmanned underwater vehicles based on a mechanical antenna," *Antennas and Propagation & USNC/URSI National Radio Science Meeting*, 1997–1998, San Diego, USA, Jul. 2017.
5. Weldon, J., K. Jensen, and A. Zettl, "Nanomechanical radio transmitter," *Physica Status Solidi (B)*, Vol. 245, No. 10, 2323–2325, 2008.
6. Liu, X. J., "A kind of antenna," patent num. ZL 200920105671.9.
7. Madanayake, A., S. Choi, and M. Tarek, "Energy-efficient Ulf/Vlf transmitters based on mechanically-rotating dipoles," *Engineering Research Conference*, 230–235, Moratuwa, Sri Lanka, May 2017.
8. Srinivas Prasad, M. N., Y. K. Huang, and Y. E. Wang, "Going beyond Chu Harrington limit: Ulf radiation with a spinning magnet array," *General Assembly and Scientific Symposium of the International Union of Radio Science (URSI GASS)*, Montreal, QC, Canada, Aug. 2017.
9. Selvin S., Prasad M. N. S., Huang Y., et al.., "Spinning magnet antenna for Vlf transmitting," *Antennas and Propagation & USNC/URSI National Radio Science Meeting*, 1477–1478, San Diego, USA, Jul. 2017.
10. Sojdehei, J. J., P. N. Wrathall, and D. F. Dinn, "Magneto-inductive (Mi) communications," *MTS/IEEE Oceans 2001. An Ocean Odyssey. Conference Proceedings (IEEE Cat. No.01CH37295)*, 513–519, Honolulu, USA, Nov. 2001.
11. Sun, Z. and I. F. Akyildiz, "Magnetic induction communications for wireless underground sensor networks," *IEEE Transactions on Antennas and Propagation*, Vol. 58, No. 7, 2426–2435, 2010.
12. Ravaud, R., G. Lemarquand, S. Babic, et al.. "Cylindrical magnets and coils: Fields, forces, and inductances," *IEEE Transactions on Magnetics*, Vol. 46, No. 9, 3585–3590, 2010.
13. Ciric, I. R., "New models for current distributions and scalar potential formulations of magnetic field problems," *Journal of Applied Physics*, Vol. 61, No. 8, 2709–2717, 1987.
14. Ravaud, R. and G. Lemarquand, "Comparison of the Coulombian and Amperian current models for calculating the magnetic field produced by radially magnetized arc-shaped permanent magnets," *Progress In Electromagnetics Research*, Vol. 95, No. 4, 309–327, 2009.
15. Kong, J. A., *Theory of Electromagnetic Waves*, EMW Publishing, Cambridge, Massachusetts, USA, 2008.
16. Perdok, U. D., B. Kroesbergen, and M. A. Hilhorst, "Influence of gravimetric water content and bulk density on the dielectric properties of soil," *European Journal of Soil Science*, Vol. 47, No. 3, 367–371, 1996.
17. Hendrickx, J. M. H., B. Borchers, D. L. Corwin, et al.. "Inversion of soil conductivity profiles from electromagnetic induction measurements," *Soil Science Society of America Journal*, Vol. 66, No. 3, 673–685, 2002.
18. Bradshaw, A. and K. Schleicher, "Electrical conductivity of seawater," *IEEE Journal of Oceanic Engineering*, Vol. 5, No. 1, 50–62, 1980.
19. Cohen, M. B., U. S. Inan, and E. W. Paschal, "Sensitive broadband Elf/Vlf radio reception with the awesome instrument," *IEEE Transactions on Geoscience and Remote Sensing*, Vol. 48, No. 1, 3–17, 2010.
20. Harriman, S. K., E. W. Paschal, and U. S. Inan, "Magnetic sensor design for femtotesla low-frequency signals," *IEEE Transactions on Geoscience and Remote Sensing*, Vol. 48, No. 1, 396–402, 2010.